Hydrothermal growth and characterization of shape-controlled NH4V3O8

Journal:	*New Journal of Chemistry*
Manuscript ID:	NJ-ART-11-2013-001446.R2
Article Type:	Paper
Date Submitted by the Author:	01-Feb-2014

Complete List of Authors:	Vernardou, Dimitra; TEI of Crete, Center of Materials Technology and Photonics Apostolopoulou, Maria; University of Crete, Department of Materials Science and Technology Louloudakis, Dimitris; TEI of Crete, Center of Materials Technology and Photonics Katsarakis, N.; Technological Educational Institute of Crete, Center of Materials Technology and Photonics Koudoumas, Emmanuel; TEI of Crete, Center of Materials Technology and Photonics

Hydrothermal growth and characterization of shape-controlled $NH_4V_3O_8$

D. Vernardou[1]*, M. Apostolopoulou[2], D. Louloudakis[1,3], N. Katsarakis[1,4], E. Koudoumas[1,5]

[1]Center of Materials Technology and Photonics, School of Applied Technology, Technological Educational Institute of Crete, 710 04 Heraklion, Crete, Greece

[2]Department of Materials Science and Technology, University of Crete, 710 03 Heraklion, Crete, Greece

[3]Department of Physics, University of Crete, 710 03Heraklion, Crete, Greece

[4]Institute of Electronic Structure and Laser, Foundation for Research & Technology-Hellas, P.O. Box 1527, Vassilika Vouton, 711 10 Heraklion, Crete, Greece

[5]Electrical Engineering Department, School of Applied Technology, Technological Educational Institute of Crete, 710 04 Heraklion, Crete, Greece

*corresponding author, e-mail dimitra@iesl.forth.gr

Abstract

The growth of ammonium trivanadate coatings was carried out on fluorine doped tin dioxide glass substrate by hydrothermal method using an aqueous solution of ammonium metavanadate and hydrochloric acid to adjust the pH. Among the various pH values, the coating grown using pH 6 at 95 ^{o}C after 2 hr exhibited the highest electrochemical activity and the fastest time response. In addition, the kinetics of lithium ions for the oxides prepared at pH 2 was found to be affected by the deposition period. These findings are discussed in terms of possible variations in crystals' shape, crystallinity and thickness occurring during the different pH and

deposition periods studied. The importance of achieving crystalline material for the best electrochemical performance is presented.

1. Introduction

The growth of vanadium oxide derivatives with well-defined morphologies has attracted intensive interest because their properties can be tuned as a function with the shape, dimensionality and size[1-7]. As an example, a large active surface area, small particle size and low density can improve the intercalation properties of the materials resulting in high diffusion coefficient and charge capacity during ion intercalation[8,9]. Therefore, it is important to investigate the growth parameters for the fabrication of crystals with controllable architectures.

Currently, research effort has been directed in ammonium trivanadate ($NH_4V_3O_8$) because of its relatively new application as intercalation material. It has high specific energy, good rate capacity and long cycle life, which makes it a promising material in lithium batteries[5]. Ammonium trivanadate with a belt-like shape has been prepared using ammonium metavanadate (NH_4VO_3) and hydrochloric or sulfuric acid to adjust the pH solution to 1.5[1]. Wang et. al. has observed that the morphology of the final product is depended on the surfactant and the water content. In particular, flakes $NH_4V_3O_8{\cdot}0.2H_2O$ are synthesized using sodium dodecyl sulfonate and sulfuric acid, while nanorods $NH_4V_3O_8{\cdot}0.37H_2O$ through sodium dodecyl benzene sulfonate and hydrochloric acid[2]. Variable morphologies including shuttles, flowers, belts and plates of $NH_4V_3O_8$ are also possible to grow using NH_4VO_3 and acetic acid at 140 ^oC for 48 hr[5]. Apart from ammonium metavanadate, vanadium pentoxide (V_2O_5) can be used with NH_3 and a mixture of NH_4Cl to form ammonium trivanadate at 140 ^oC for 48 hr[6].

In most cases, one may observe that long deposition periods > 36 hr, temperatures ≥ 130 ^{o}C and surfactants are required to get $NH_4V_3O_8$ with different morphologies.

In this work, we have used the hydrothermal process for the growth of $NH_4V_3O_8$ coatings on fluorine doped tin dioxide (FTO) glass substrates using NH_4VO_3 in water and hydrochloric acid to adjust the pH of the solution. Based on the previous reports, we focused on studying the effect of pH and deposition period to modify the morphological characteristics of the final products at 95 ^{o}C for ≤ 2 hr without the use of surfactants. We finally comment on the most suitable processes in terms of producing potentially useful intercalation materials.

2. Experimental

2.1 Synthesis

The hydrothermal growth of $NH_4V_3O_8$ coatings was performed on fluorine doped tin dioxide glass (2 x 2 cm) using an aqueous solution of NH_4VO_3 and HCl to adjust the pH. The solution preparation involved the stirring of 100 ml, H_2O and 0.48 g NH_4VO_3 with the pH solution adjustment to 2, 4, 5 and 6. Then, the yellow suspension was placed in a Pyrex glass bottle with polypropylene autoclavable screw cap, with the substrate positioned on the bottom and heated at 95 ^{o}C for 2 hr in a regular laboratory oven. After the end of the deposition period, the bottle was allowed to cool to room temperature. Finally, the samples (regarded as the substrate with the $NH_4V_3O_8$ coating on the top) were washed with water and dried in air at 95 ^{o}C.

2.2 Characterization

X-ray diffraction (XRD) measurements were carried out in different positions on the samples using a Siemens D5000 Diffractometer for 2θ = 10.0-50.0 ^{o}, step size 0.05 ^{o} and step time 60 s/^{o}. Raman characterization was performed in a Nicolet Almega XR micro-Raman system using the 780 nm line for a range of 100-1100 cm^{-1}. Finally, surface imaging was accomplished in a Jeol JSM-6390LV electron microscope. Finally, optical measurements were done in a Perkin-Elmer Lambda 950 UV-vis spectrophotometer in the wavelength range of 300-900 nm.

2.3 Electrochemical evaluation

Even though, Li is a suitable counter and reference electrode for the electrochemical measurements of the coatings, for comparative purposes with previous work[10-16], platinum and Ag/AgCl were used as counter and reference electrodes respectively in this work. The measurements were accomplished in 1 M $LiClO_4$/propylene carbonate solution, which acted as the electrolyte, using a scan rate of 20 mV s^{-1} through the voltage range of –1000 mV to +1000 mV. Propylene carbonate was selected as a solvent because its high dielectric constant contributes to increased charge density[17]. All samples were scanned for 1, 100 and 250 times. Finally, the lithium intercalation/extraction process with respect to time was studied using chronoamperometry at -1000 mV and +1000 mV for a step of 200 s.

3. Results and discussion

3.1 Structure

Fig. 1 presents the XRD pattern of the NH_4VO_3 powder. All diffraction peaks of the powder are indexed to orthorhombic NH_4VO_3[18]. In addition, the as-prepared

coatings for pH 4 and 6 show features at 11.4 ^{o} and 22.8 ^{o} with corresponding Miller indices (001) and (002), which are correlated with a monoclinic $NH_4V_3O_8$ crystal structure (Fig. 1)[2,5]. Since all patterns did not give sufficient number of reflections for the calculation of the cell parameters, the Miller indices were then assigned based on the literature. Furthermore, the data related with the pH 2 samples indicate one weak peak at 11.4 ^{o} (001) due to the monoclinic ammonium trivanadate crystal structure and peaks at 26.5, 33.7 and 37.5 ^{o} with Miller indices (110), (101) and (200) respectively due to the underlying substrate[19] indicating their low crystallinity (Fig. 1 inset). XRD patterns presented the $NH_4V_3O_8$ phase along the surface indicating the products are of high quality. However, it is noticed that the intensity of (001) peak becomes stronger upon increasing the pH value to 6 implying that the degree of crystallinity is enhanced. Based on the literature reporting many studies related with the growth of crystalline and amorphous coatings, a possible candidate to intercalate larger amounts of lithium could be the low crystalline quality coatings (pH 2). This happens due to the more open structure[5,20-22], high cycle performance and charge capacity since no phase transformations occur during intercalation and deintercalation processes[23,24] for the low crystalline or amorphous materials.

In this work, the structure of coatings grown at different pH values is such that the (001) planes lying parallel to the substrate. Based on the two reflections observed i.e. (001) and (002), the lattice constant b was calculated to be equal to 8.4232 Å, which is in agreement with the literature (JCPDS card no. 88-1473 card)[7].

The characteristics of the samples can also be influenced by the deposition time. Towards this scope, the growth time was decreased from 2 hr to 30 min, since deposition period below 30 min resulted in coatings with poor surface coverage (i.e. no efficient coverage of the substrate by the coating). Based on consideration of

similar procedures[1,2,25] that the pH 2 provides $NH_4V_3O_8$ structures with satisfactory electrochemical performance, the effect of the deposition period was focused on this pH value for the determination of the conditions that can possibly lead to respective structures obtained in the literature. We have found that the structure of the grown coatings does not depend upon the reaction time, since there was no evidence of diffraction peaks apart from those correlated with the underlying substrate (not shown here for brevity).

Fig. 2 shows the Raman spectra of the NH_4VO_3 powder and the $NH_4V_3O_8$ coating grown for pH 6. The Raman spectrum of NH_4VO_3 consists of a strong band at 926 cm^{-1}, medium peak at 645 cm^{-1} and weak bands at 209, 259, 493 and 895 cm^{-1}, which are in a good agreement with the literature[5]. Regarding the spectrum of $NH_4V_3O_8$, presents bands at 963 and 993 cm^{-1} assigned to V=O stretching modes of distorted octahedral and distorted square pyramids respectively. The peak at 813 cm^{-1} corresponds to V-O stretching bonds[26]. The bands at 556 and 670 cm^{-1} are attributed to V-O-V stretching modes. Finally, a very strong band at 670 cm^{-1} confirms predominantly the existence of a chain-like structure similar to NH_4VO_3[27]. Other bands in the frequency range below 400 cm^{-1} are assigned to V-O and N-H bending modes[28].

For pH < 6, the Raman peaks were lower in intensity and broader. One may then say that the results derived from the XRD and micro-Raman spectroscopy are in full agreement confirming the pH and therefore the acidity of the solution dependence on the structure. In terms of the samples deposited at different periods, there were no evident variations among them. In the case of pH 2 sample, the simultaneous presence of well-identified Raman bands with the absence of XRD peaks suggests that it is mainly amorphous retaining however a short-range crystalline ordering[29].

3.2 Morphology

Figs. 3 (a), (b), (c) and (d) present SEM images of the as-prepared samples for 2 hr at pH 2, 4, 5 and 6 respectively. One can observe that platelet microcrystals are formed and their shape is dependent upon the acidity of the solution. Rectangular-, hexagonal- and rhombohedral-shaped crystals are obtained for pH 2, 4, 5 and 6.

Figs. 4 (a) and (b) show the images of the crystals grown for 30 min and 1 hr respectively at pH 2. It can be seen that there is no obvious influence of the reaction time on the shape of the final products apart from a larger size and sparsely distributed crystals at higher deposition periods (2 hr). In this case, the transmittance decreases for lower growth periods i.e. 0.65, 0.40 and 0.30 at 500 nm for 2 hr, 1 hr and 30 min respectively, which may be related with the samples thickness 's increase. This suggests that the growth mechanism for the longer deposition periods is an interplay of deposition and dissolution processes. In particular, for reaction time of 2 hr, their size and thickness are ca. 6 μm and ca. 650 nm respectively decreasing to ca. 5 μm and ca. 330 nm for the 30 min sample.

In all cases, the crystals cover the whole surface of the substrate, but they do not form a continuous layer.

In order to understand the pH-dependence of the crystallite morphology, the growth mechanism is considered based on observations in the literature for 1D and 2D $NH_4V_3O_8$ crystal growth[5,30]. The basic reaction for the synthesis of ammonium trivanadate microcrystals can be formulated below:

$$3NH_4VO_3 + HCl \leftrightarrow NH_4V_3O_8 + NH_3 + NH_4Cl + H_2O$$

At the initial stage, adding the acid to the aqueous solution of NH_4VO_3, vanadium polyanion units surrounded by dipolar water molecules are formed due to the

protonation of ammonium metavanadate[31]. These units are coordinated with other water molecules, the number of which depends on the pH value leading to different forms of vanadium precursors. Then the condensation of the vanadium precursors can go either via olation or oxolation process as shown below[30]

Olation V-OH + -V-OH_2 → -V-OH-V- + H_2O (fast)

Oxolation V-OH + HO-V- → -V-O-V- + H_2O (slow)

They both involve the nucleophilic addition of negatively charged OH^- groups onto positive vanadium cations. Hydroxo V-OH groups are then required for condensation to occur. However, olation reactions, in which water molecules are already formed, are kinetically faster than oxolation reactions.

In our case, the condensation probably occurs via oxolation in the *xy* plane along the V-OH leading to plate-like 2D microcrystals. One may then say that there are no H_2O-V-OH groups present within the *xy* plane to support 1D belt- or shuttle-like structure[5].

To summarize, tuning the pH value can be used to control the shape of $NH_4V_3O_8$ microplates from rectangular up to hexagonal and rhombohedral. Further increase of the pH is not possible because the acidity of the pure aqueous NH_4VO_3 solution is around 6.4.

3.3 Electrochemical behaviour

3.3.1 Cyclic voltammetry

In order to examine the effect of the pH on the electrochemical performance of the coatings including stability and reversibility, cyclic voltammetry experiments were conducted as shown in Fig. 5. The potential was ranged from -1000 mV to +1000 mV at a scan rate of 20 mV s^{-1}. The as-grown coating for pH 6 presents one cathodic peak

at -240 mV and one symmetric anodic peak. These are attributed to Li^+ intercalation and extraction accompanying gain and loss of an e^- respectively[32]. The presence of the symmetric peaks reveals that the electrochemical process is highly reversible. Furthermore, it becomes evident that the current density of the pH 6 is the highest of all others indicating an enhanced electrochemical activity. On the other hand, the pH 4 and 5 samples exhibit less distinctive cathodic and anodic peaks, which may be due to the lack of requisite ion injection sites. One may then suggest that the amount of incorporated charge is smaller for the lower (hexagonal crystals) compared with the higher (rhombohedral crystals) crystalline quality samples. Hence, the highest electrochemical activity may be a combination of both structure and morphology. For number of scans > 20, no anodic or cathodic peaks were discerned in the cyclic voltammogram curves and the sweeping area was decreased significantly suggesting poor electrochemical stability of the samples due to observed dissolution of the coatings by the electrolyte.

There was a noticeable difference in the cyclic voltammogram curves for the pH 2 coating. The shape of the curve is different compared with the pH 6 and two less distinctive cathodic and anodic peaks appear at -200 mV (1) and +200 mV (2) respectively as indicated in Fig. 5 inset. This discrepancy compared with the rest of the samples may due to the existence of amorphous $NH_4V_3O_8$. Long-term degradation was also observed for this one after the 20^{th} scan as evident from the reduction of the sweeping area and the disappearance of the peaks (not shown here). Furthermore, a decrease of current density by three degrees of magnitude was observed in comparison with the pH 6. This is consistent with reports that amorphous materials dissolve more easily than crystallized ones during continuous lithium ion intercalation / extraction processes[33,34].

The kinetic process of lithium ion incorporation for the pH 2 coating can be affected by the deposition period as shown in Fig. 6. It is observed that the peak intensities and the sweeping area are higher for the 30 min coating with no obvious shift compared with the 2 hr sample suggesting the reversible oxidation and reduction of the $NH_4V_3O_8$. This behaviour is ought to the larger thickness of the 30 min incorporating higher number of lithium ions inside the structure.

3.3.2 Switching response

To calculate the amount of lithium interchanged between the $NH_4V_3O_8$ and the electrolyte[10], chronoamperometry measurements were performed switching the potential between -1000 mV and +1000 mV at an interval of 200 s as indicated in Fig. 7. We estimated that the extracted is lower than the intercalated charge for all samples indicating that lithium ions remain in the oxide. The amount of intercalation charge for the pH 6 was calculated to be 50 mC cm^{-2}, i.e. ten times larger compared with the one grown at pH 2. This value is higher than the sputtered[35], aqueous sol-gel[36], electrodeposited[11] and atmospheric pressure chemical vapor deposited[10] V_2O_5. We therefore note that the hydrothermally grown $NH_4V_3O_8$ crystals produced in this work are of comparable efficiency to intercalation material prepared by more complicated techniques.

In addition, the time response[10] (t_c) for the pH 6 sample was calculated to be 37 ± 1 s and 9 ± 1 s for the lithium intercalation and extraction respectively. On the other hand, the t_c for the pH 2 was 55 ± 1 s (lithium intercalation) and 20 ± 1 s (lithium extraction). Regarding, the samples grown for different deposition periods at pH 2, the 30 min sample presented time constant of 45 ± 1 s (intercalation) and 15 ± 1 s

(extraction). Cation reaction with 30 min sample is therefore faster compared to 2 hr sample grown using the same pH value.

In all cases, the extraction process is quicker than the intercalation, which is in agreement with others[37-39].

4. Conclusions

Ammonium trivanadate coatings were grown using hydrothermal procedure at 95 ^{o}C for 2 hr controlling the pH of the solution. The shape of the crystals is strongly dependent on the acidity of the solution promoting rectangular, hexagonal and rhombohedral microcrystals for pH 2, 4 and 6 respectively. The pH 6 samples presented enhanced lithium intercalation / extraction performance in both charge storage and response time. This is correlated with the crystalline nature of $NH_4V_3O_8$ and consequently the morphological properties of the samples. In addition, the lithium ion kinetics at pH 2 was improved lowering the deposition period to 30 min possibly due to the increased thickness of the coating. This relatively simple and low-cost hydrothermal route can be significant for the production of $NH_4V_3O_8$ microcrystals with controlled shape and morphology as high performance intercalation materials.

Acknowledgements

This project is implemented through the Operational Program "Education and Lifelong Learning", action Archimedes III and is co-financed by the European Union (European Social Fund) and Greek national funds (National Strategic Reference Framework 2007 - 2013).

References

[1] L. Q. Mai, C. S. Lao, B. Hu, J. Zhou, Y. Y. Qi, W. Chen, E. D. Gu and Z. L. Wang, *J. Phys. Chem. B*, 2006, **110***,* 18138.

[2] H. Wang, K. Huang, S. Liu, C. Huang, W. Wang and Y. Ren, *J. Power Sources,* 2011, **196**, 788.

[3] H. Wang, Y. Ren, W. Wang, X. Huang, K. Huang, Y. Wang and S. Liu, *J. Power Sources,* 2012, **199**, 315.

[4] H. –K. Park, G. Kim, *Solid State Ionics,* 2010, **181**, 311.

[5] G. S. Zakharova, Ch. Täschner, T. Kolb, C. Jähne, A. Leonhardt, B. Büchner and R. Klingeler, *Dalton Trans.,* 2013, **42**, 4897.

[6] S. D. Huang, *Chem. Commun.,* 1998, 1069.

[7] S. G. Leonardi, P. Primerano, N. Donato and G. Neri, *J. Solid State Chem.,* 2013, **202**, 105.

[8] Y. Wang, K. Takahashi, H. Shang and G. Cao, *J. Phys. Chem. B,* 2005, **109**, 3085.

[9] J. -K. Lee, G. -P. Kim, I. K. Song and S. -H. Baeck, *Electrochem. Commun.,* 2009, **11**, 1571.

[10] D. Vernardou, H. Drosos, E. Spanakis, E. Koudoumas, C. Savvakis and N. Katsarakis, *J. Mater. Chem.,* 2011, **21**, 513.

[11] D. Vernardou, A. Sapountzis, E. Spanakis, G. Kenanakis, E. Koudoumas and N. Katsarakis, *J. Electrochem. Soc.,* 2013, **160**, D6.

[12] D. Vernardou, P. Paterakis, H. Drosos, E. Spanakis, I. M. Povey, M. E. Pemble, E. Koudoumas and N. Katsarakis, *Sol. Energ. Mat. Sol. C,* 2011, **95**, 2842.

[13] H. Drosos, A. Sapountzis, E. Koudoumas, N. Katsarakis and D. Vernardou, *J. Electrochem. Soc.,* 2012, **159**, E145.

[14] I. Turhan, F. Z. Tepehan and G. G. Tepehan, *J. Mater. Sci.,* 2012, **40**,1359.

[15] Z. Wang, J. Chen and X. Hu, *Thin Solid Films,* 2000, **375**, 238.

[16] M. B. Sahana, C. Sudakar, C. Thapa, G. Lawesa, V. M. Naik, R.J. Baird, G. W. Auner, R. Naik and K. R. Padmanabhan, *Mater. Sci. Eng. B.,* 2007, **143**, 42.

[17] M. Inagaki, H. Konno and O. Tanaike, *J. Power Sources*, 2010, **195**, 7880.

[18] J. Ding, G. Li and H. Peng, *J. Exp. Nanosci.,* 2012, **7**, 485.

[19] E. Elangovan, K. Ramamurthi, *Thin Solid Films,* 2005, **476**, 231.

[20] G. Pistoia, M. Pasquali, G. Wang and L. Li, *J. Electrochem. Soc.,* 1990, **137,** 2365.

[21] J. Scarminio, A. Tolledo, A. A. Andersson, S. Passerini and F. Decker, *Electrochim. Acta*, 1993, **38,** 1637.

[22] F. Coustier, S. Passerini and W. H. Smyrl, *Solid State Ionics*, 1997, **100**, 247.

[23] Y. S. Yoon, J. S. Kim and S. H. Choi, *Thin Solid Films*, 2004, **460**, 41.

[24] D. M. Yu, S. T. Zhang, D. W. Liu, X. Y. Zhou, S. H. Xie, Q. F. Zhang, Y. Y. Liu and G. Z. Cao, *J. Mater. Chem.,* 2010, **20**, 10841.

[25] Ch. V. S. Reddy, K. –I. Park, S. –I. Mho, I. –H. Yeo and S. –M. Park, *Bull. Korean Chem. Soc.,* 2008, **29**, 2061.

[26] L. V. Kristallov, O. V. Koryakova, L. A. Perelyaeva and M. T. Tsvetkova, *Russ. J. Inorg. Chem.,* 1987, **32**, 1811.

[27] A. Shimizu, T. Watanabe and M. Inagaki, *J. Mater. Chem.,* 1994, **4**, 1475.

[28] J. Twu, C.-F. Shih, T.-H. Guo and K.-H. Chen, *J. Mater. Chem.,* 1997, **7**, 2273.

[29] J. Zhang, M. Li, Z. Feng, J. Chen and C. Li, *J. Phys. Chem. B*, 2006, **110**, 927.

[30] J. Livage, *Materials,* 2010, **3**, 4175.

[31] B. Li, Y. Xu, G. Rong, M. Jing and Y. Xie, *Nanotechnology,* 2006, **17,** 2560

[32] K. Lee and G Cao**,** *J. Phys. Chem. B*, 2005, **109***,* 11880.

[33] S. H. Ng, S. Y. Chew, J. Wang, D. Wexler, Y. Tournayre, K. Konstantinov and H. K. Liu, *J. Power Sources,* 2007, **174**, 1032.

[34] T. C. Arnoldussen, *J. Electrochem. Soc.,* 1981, **128**, 117.

[35] K. S. Ahn, Y. C. Nah, J. H. Yum and Y.-E. Sung, *Jpn. J. Appl. Phys.,* 2002, **41**, L212.

[36] M. Benmoussa, A. Outzourhit, A. Bennouna and E. L. Ameziane, *Thin Solid Films,* 2002, **405**, 11.

[37] Y. Fujita, K. Miyazaki and C. Tatsuyama, *Jpn. J. Appl. Phys.,* 1985, **24**, 1082.

[38] M. Denesuk, J. P. Cronin, S. R. Kennedy and D. R. Uhlmann, *J. Electrochem. Soc.,* 1997, **144**, 1971.

[39] D. Louloudakis, D. Vernardou, E. Spanakis, N. Katsarakis and E. Koudoumas, *Surf. Coat. Technol.,* 2013, **230**, 186.

Fig. Captions

Fig. 1. XRD of the NH_4VO_3 powder and the as-prepared hydrothermally grown samples for pH 2 (inset), pH 4 and pH 6 at 95 ^oC for 2 hr. FTO peaks are denoted with black dots.

Fig. 2. Raman spectra of the NH_4VO_3 powder and the $NH_4V_3O_8$ coating grown at 95 ^oC for pH 6.

Fig. 3. SEM images of the $NH_4V_3O_8$ grown for (a) pH 2, (b) pH 4, (c) pH 5 and (d) pH 6.

Fig. 4. SEM images of the samples grown at pH 2 for (a) 30 min and (b) 1 hr.

Fig. 5. Cyclic voltammograms of the first scan for the pH 2 with its magnification as inset, pH 4 and pH 6 using a scan rate of 20 mV s^{-1}. Electrode active area was 1 cm^2.

Fig. 6. Cyclic voltammograms of the first scan for the 30 min and 1 hr at pH 2 using a scan rate of 20 mV s^{-1}. Electrode active area was 1 cm^2.

Fig. 7. The chronoamperometric response recorded at a potential step of -1000 mV and +1000 mV for a time step of 200 s in 1 M $LiClO_4$ / polypropylene carbonate as an electrolyte for the pH 2 (30 min samples as inset), pH 4 and pH 6 samples grown at 95 ^oC for 2 hr.

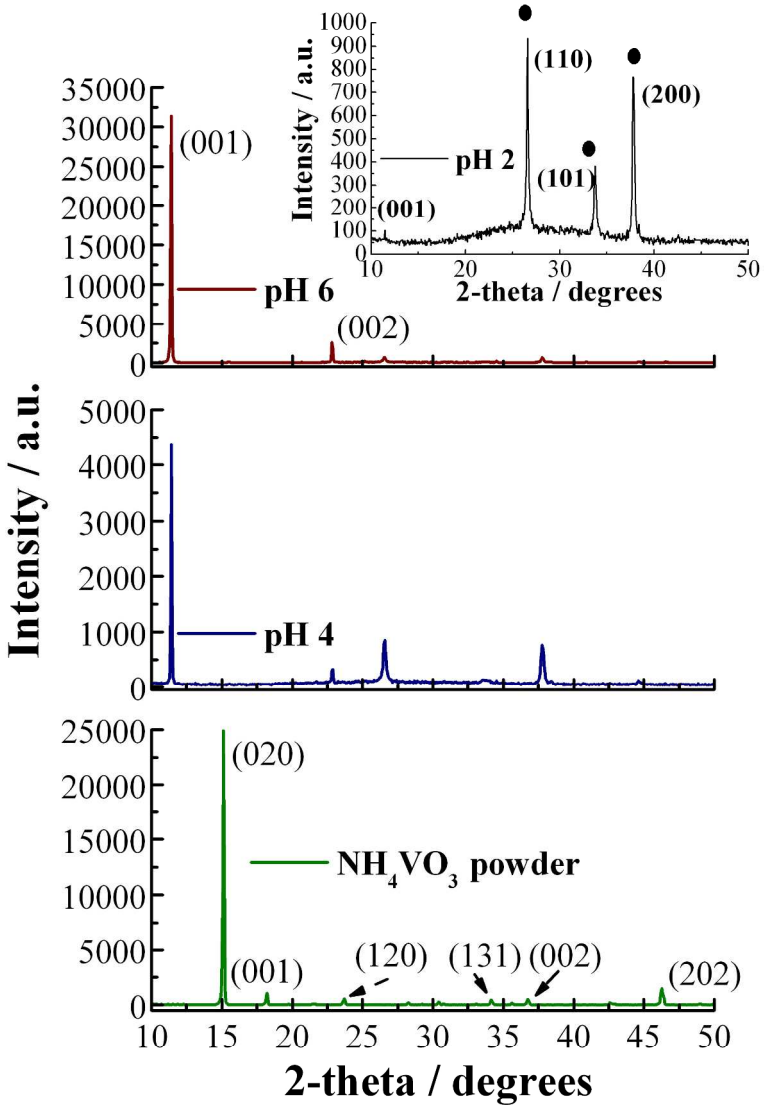

210x297mm (300 x 300 DPI)

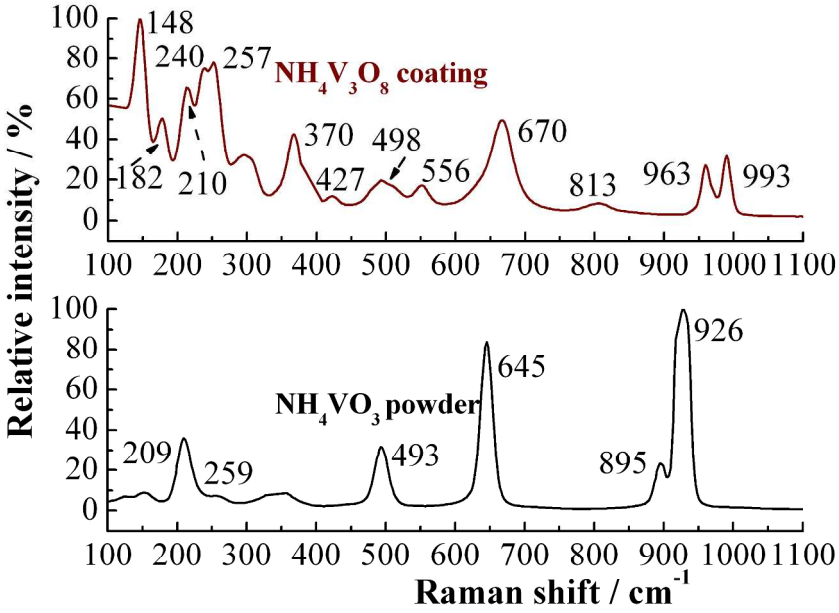

297x210mm (300 x 300 DPI)

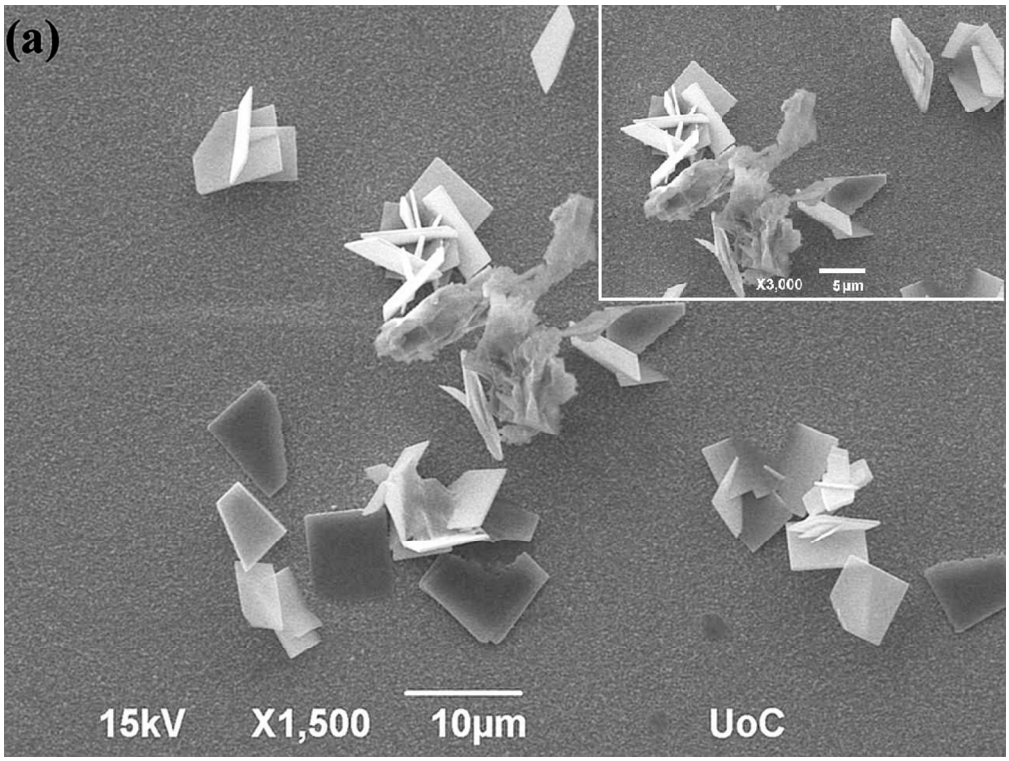

338x254mm (96 x 96 DPI)

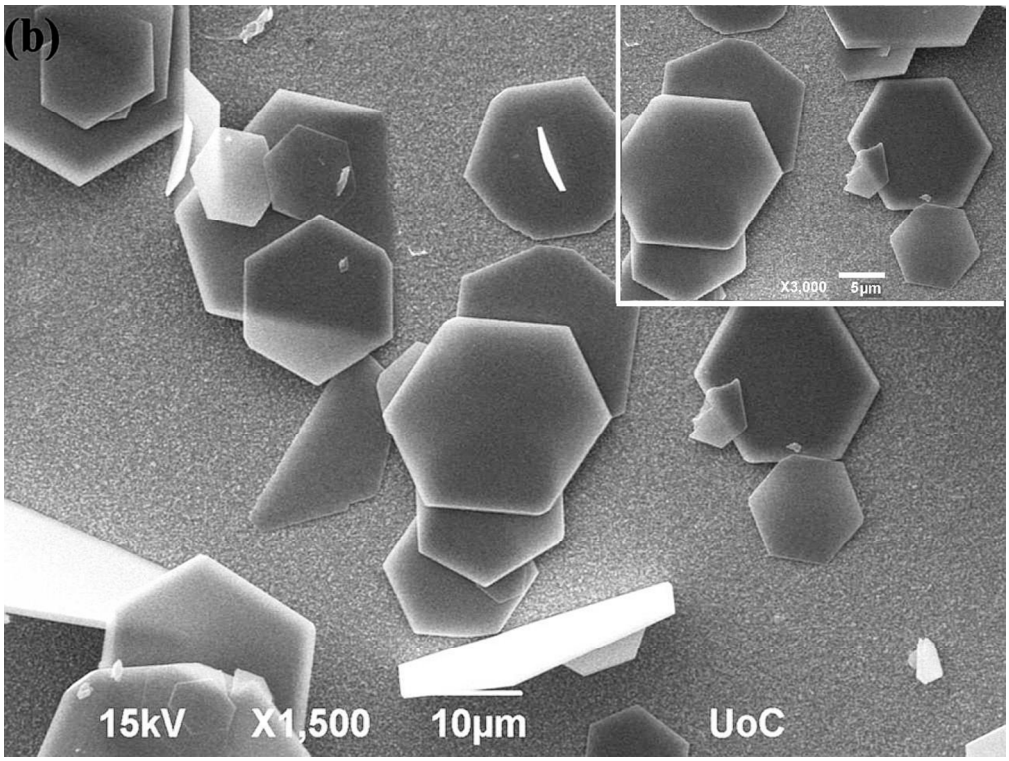

338x254mm (96 x 96 DPI)

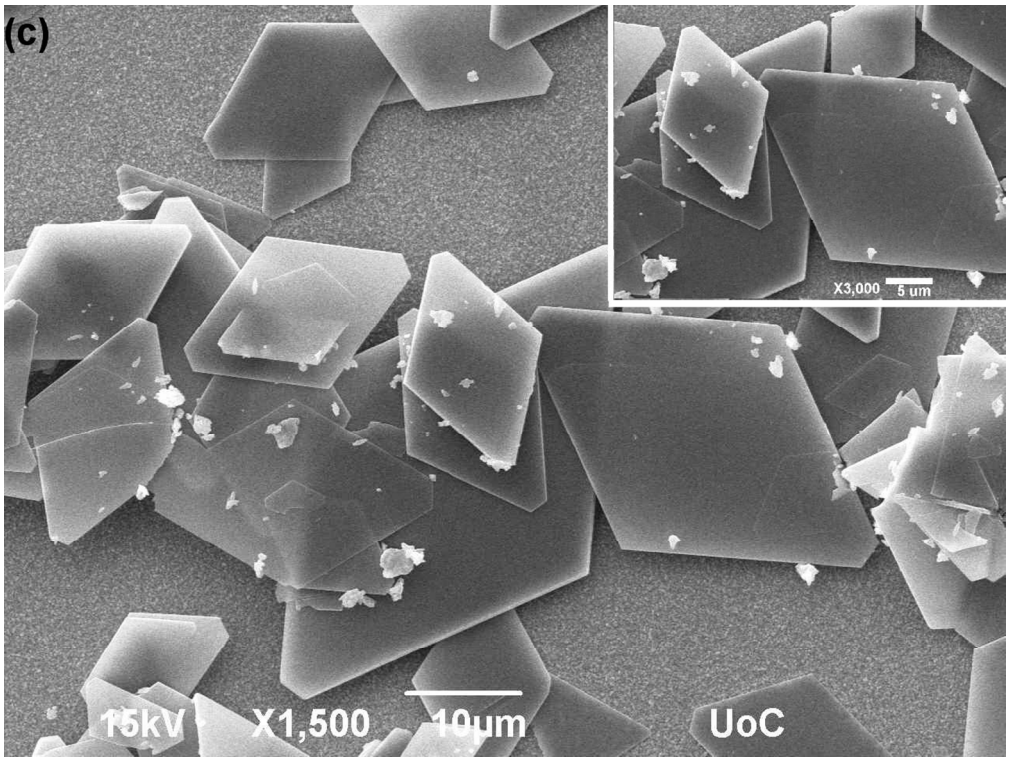

338x254mm (96 x 96 DPI)

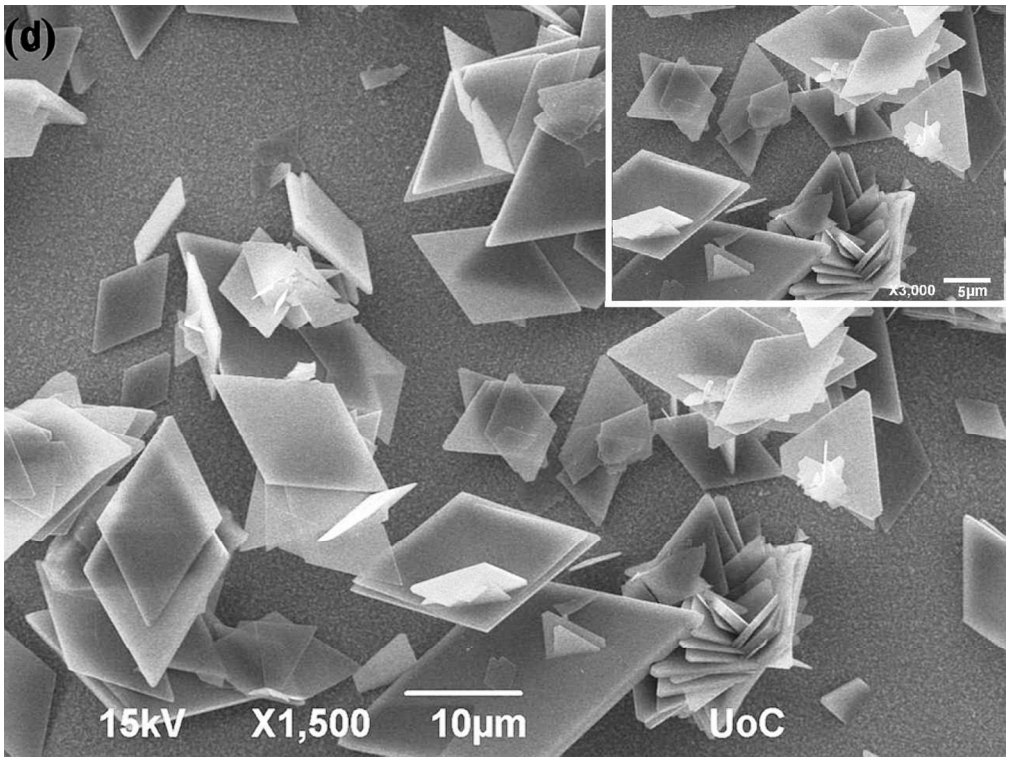

338x254mm (96 x 96 DPI)

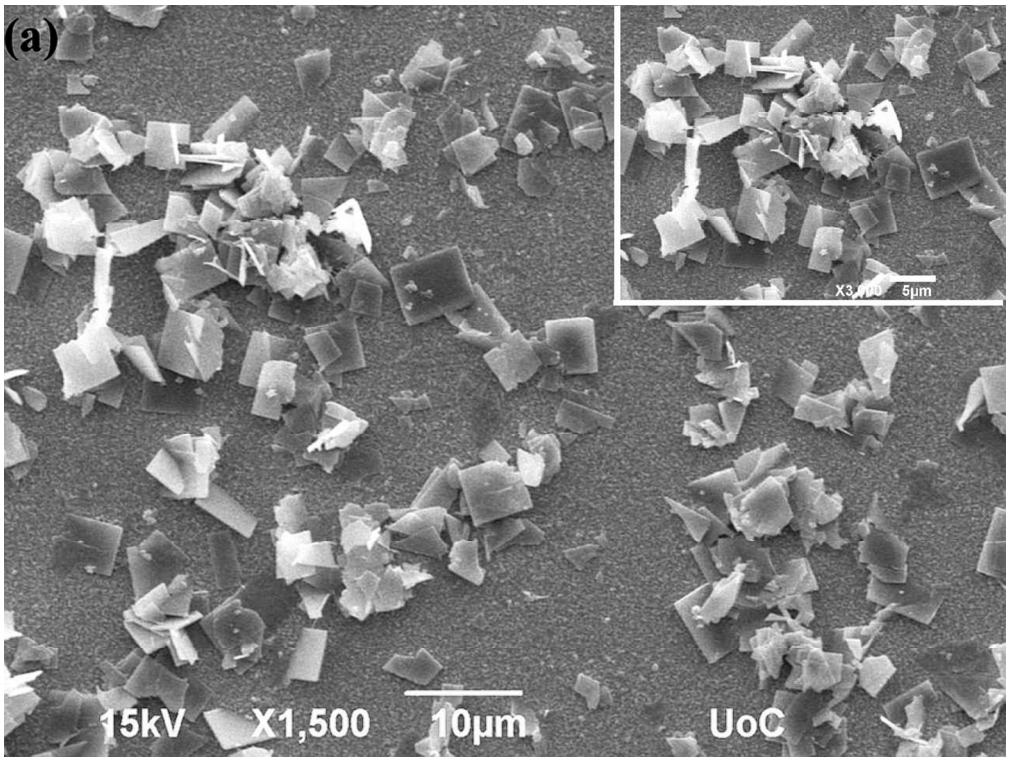

338x254mm (96 x 96 DPI)

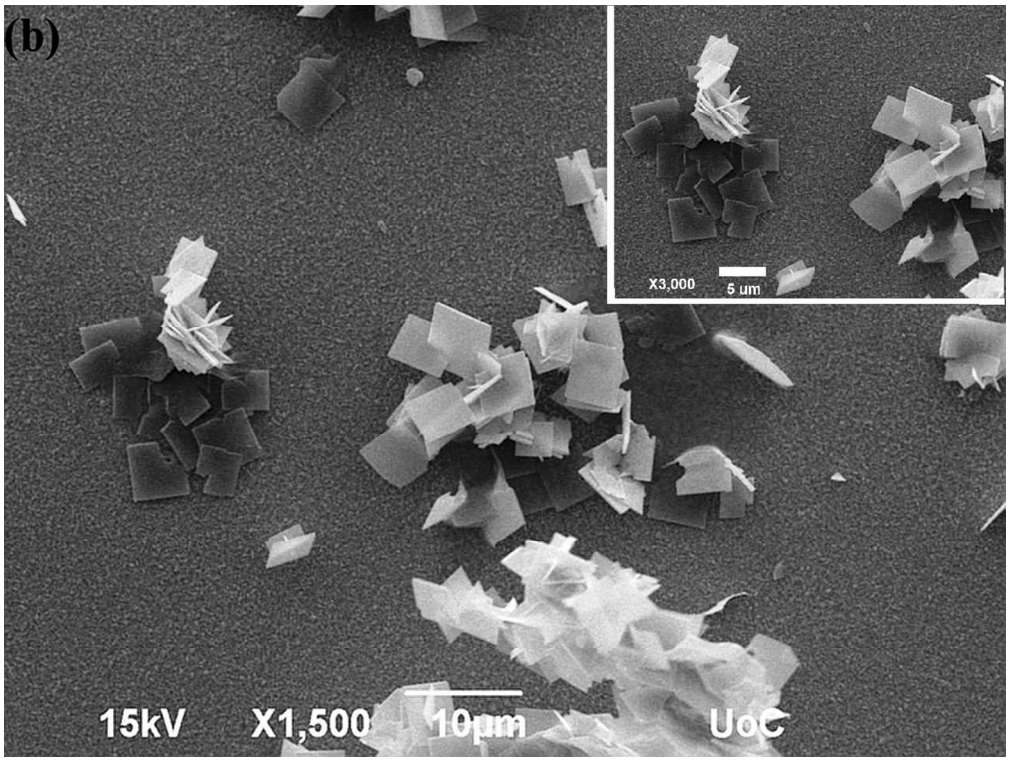

338x254mm (96 x 96 DPI)

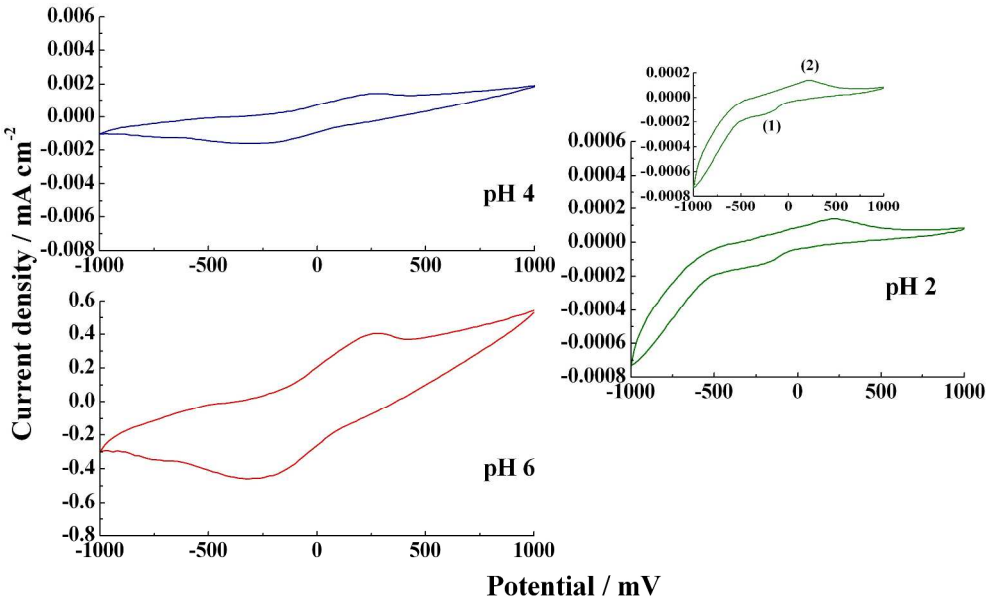

273x165mm (300 x 300 DPI)

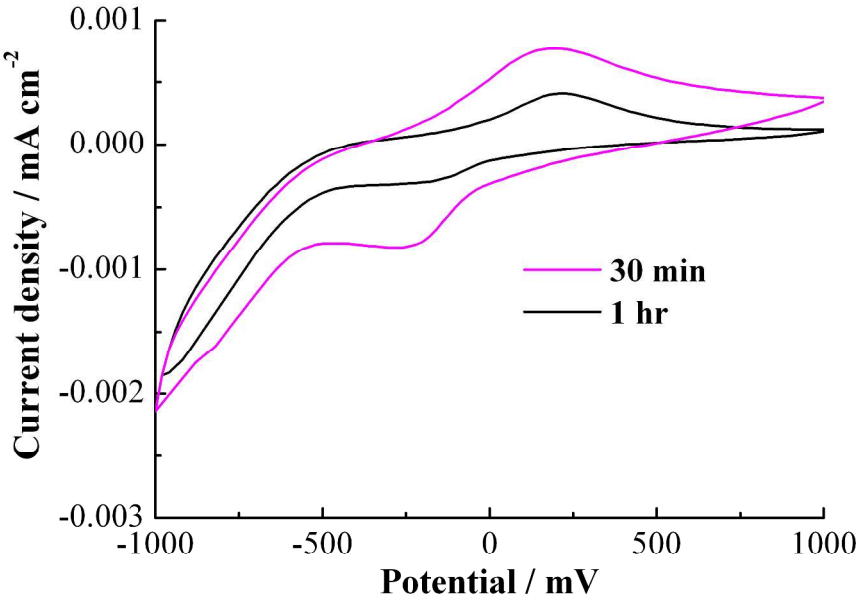

297x210mm (300 x 300 DPI)

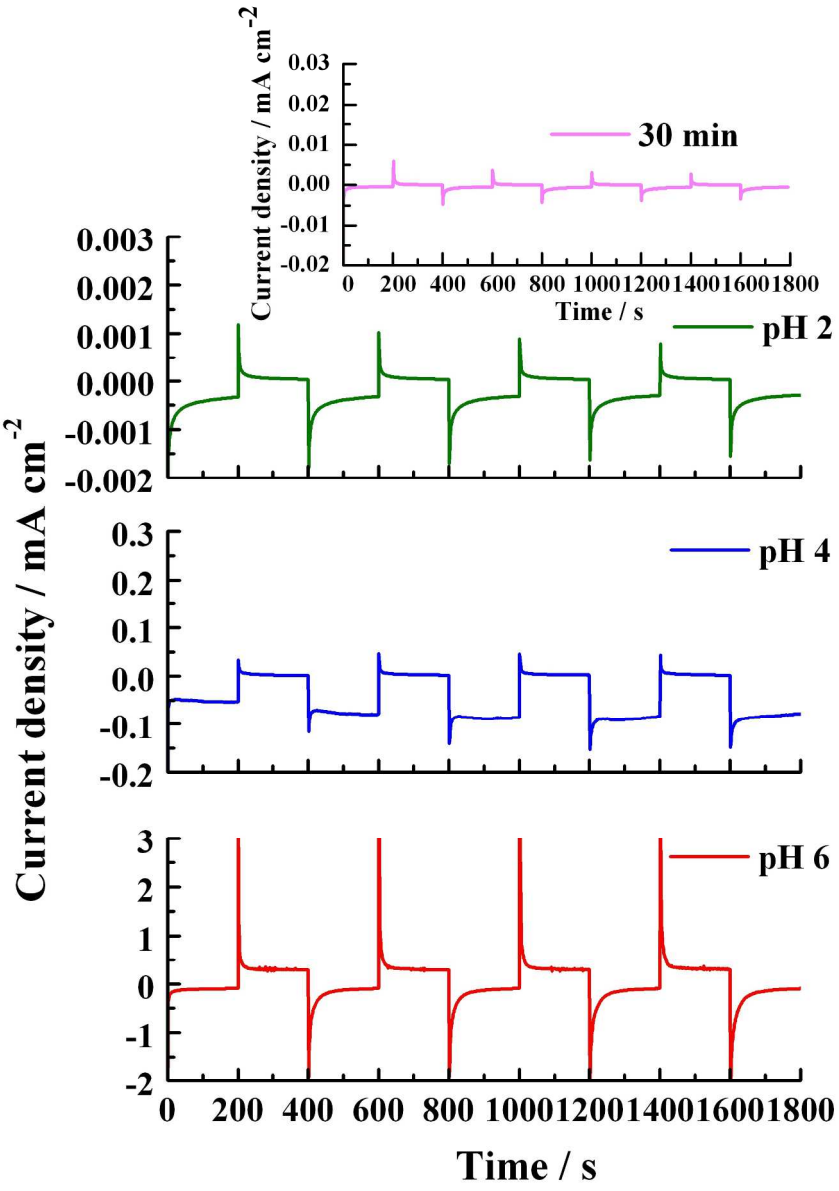

189x270mm (300 x 300 DPI)

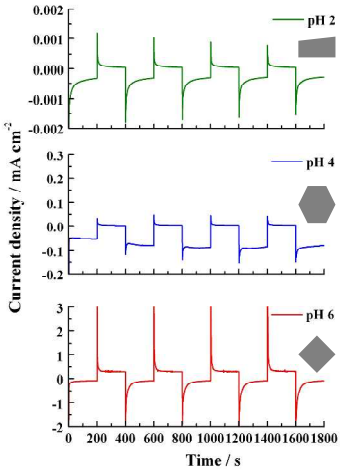

The acidity of the solution can alter the crystal's shape and structure of the coatings grown at 95 ^{o}C controlling their electrochemical performance.